Atmospheric Environment 95 (2014) 71–81

Contents lists available at ScienceDirect

Atmospheric Environment

journal homepage: www.elsevier.com/locate/atmosenv

An empirical method of RH correction for satellite estimation of ground-level PM concentrations

Zifeng Wang [a], Liangfu Chen [a,*], Jinhua Tao [a], Yang Liu [b], Xuefei Hu [b], Minghui Tao [a]

[a] State Key Laboratory of Remote Sensing Science, Jointly Sponsored by Institute of Remote Sensing and Digital Earth of Chinese Academy of Sciences and Beijing Normal University, Beijing 100101, China
[b] Rollins School of Public Health, Emory University, Atlanta, GA 30322, USA

HIGHLIGHTS

- It characterizes the aerosol hygroscopicity only using in-situ visibility, RH and PM.
- Able to account for the spatio-temporal variations of aerosol types and properties.
- Correlations between satellite AOD and PM are greatly improved by RH correction.
- Significantly extends the spatial and temporal coverage of accurate RH correction.

ARTICLE INFO

Article history:
Received 23 October 2013
Received in revised form
7 May 2014
Accepted 8 May 2014
Available online 14 May 2014

Keywords:
Hygroscopic growth model
RH correction
Particulate matters
Satellite retrieval

ABSTRACT

A hygroscopic growth model suitable for local aerosol characteristics and their temporal variations is necessary for accurate satellite retrieval of ground-level particulate matters (PM). This study develops an empirical method to correct the relative humidity (RH) impact on aerosol extinction coefficient and to further derive PM concentrations from satellite observations. Not relying on detailed information of aerosol chemical and microphysical properties, this method simply uses the in-situ observations of visibility (VIS), RH and PM concentrations to characterize aerosol hygroscopicity, and thus makes the RH correction capable of supporting the satellite PM estimations with large spatial and temporal coverage.

In this method, the aerosol average mass extinction efficiency (α_{ext}) is used to describe the general hygroscopic growth behaviors of the total aerosol populations. The association between α_{ext} and RH is obtained through empirical model fitting, and is then applied to carry out RH correction. Nearly one year of in-situ measurements of VIS, RH and PM10 in Beijing urban area are collected for this study and RH correction is made for each of the months with sufficient data samples. The correlations between aerosol extinction coefficients and PM10 concentrations are significantly improved, with the monthly correlation R^2 increasing from 0.26–0.63 to 0.49–0.82, as well as the whole dataset's R^2 increasing from 0.36 to 0.68. PM10 concentrations are retrieved through RH correction and validated for each season individually. Good agreements between the retrieved and observed PM10 concentrations are found in all seasons, with R^2 ranging from 0.54 in spring to 0.73 in fall, and the mean relative errors ranging from −2.5% in winter to −10.8% in spring. Based on the satellite AOD and the model simulated aerosol profiles, surface PM10 over Beijing area is retrieved through the RH correction. The satellite retrieved PM10 and those observed at ground sites agree well with each other, with $R^2 = 0.46$ and a relative error of 19.3%.

1. Introduction

Although ground-based measurements can provide precise information of particulate matters (PM) concentration and composition, the limited number and sparse distribution of the monitoring sites make it difficult to study the long-range transport and regional distribution of PM pollutions. Benefiting from the large spatial and long-term coverage, satellite remote sensing have been widely applied in air quality observations in recent years (Hoff and Christopher, 2009; Martin, 2008). Both theoretical analysis and observations have demonstrated the link between satellite retrieved aerosol optical depth (AOD) and surface PM concentrations. However, this AOD–PM relationship may vary greatly with

* Corresponding author. Room A203, Institute of Remote Sensing and Digital Earth, CAS, Datun Road Jia 20, Chaoyang District, Beijing 100101, China.
E-mail addresses: wangzf@radi.ac.cn (Z. Wang), princepeak@hotmail.com (L. Chen).

http://dx.doi.org/10.1016/j.atmosenv.2014.05.030
1352-2310/

location and time due to the changes of aerosol chemical and physical properties and meteorological conditions, among which the vertical structure and hygroscopicity of aerosols are two major contributors to the uncertainties involved. Accordingly, the satellite estimation of PM should include two significant steps, which are connected by the ground-level aerosol extinction coefficient (b_{ext}) (Wang et al., 2010). The first step is to extract b_{ext} from AOD through vertical correction, and the second step is to reduce the hygroscopic growth impact on b_{ext}, so as to improve its correlation with PM concentration. Many studies implemented vertical corrections on satellite AOD before estimating PM, using planetary boundary layer (PBL) height (Koelemeijer et al., 2006; Wang et al., 2010; Zheng et al., 2013) or aerosol vertical profiles (Hutchison et al., 2008; X. Liu et al., 2009; Y. Liu et al., 2009, 2011), both of which can be measured by LIDAR or simulated by atmospheric models. This study will focus on the RH impact on the b_{ext}–PM correlation, and develop a new method for the second step mentioned above.

According to Hand and Malm (2007), the hygroscopic characteristics of aerosols are determined by their chemical composition, mixture status and size distribution, and have large spatial and temporal variations. Hence the accurate information of aerosol hygroscopicity will be the basis of effective RH correction. When accounting for the hygroscopic growth impact, some studies simply use RH as one of the predictor variables in a multivariate regression model (Liu et al., 2005; Pelletier et al., 2007; Tian and Chen, 2010), which does not fully address the non-linear particle growth patterns and can only represent an "average" RH impact on the AOD–PM relationship for the whole dataset. Other researchers use a single uniform function of aerosol hygroscopic growth factor (e.g. f(RH)) to conduct RH correction (Li et al., 2005; Koelemeijer et al., 2006; Guo et al., 2009), which are not sufficient to characterize the spatial and temporal changes of aerosol hygroscopicity. Liu et al. (2005) and Donkelaar et al. (2006) utilize the model simulated AOD–PM relationship to directly convert satellite AOD into surface PM concentration. Though simultaneously accounting for the aerosol vertical profiles and hygroscopic growth, this approach is still limited by the simulation uncertainty and the coarse spatial resolution of models. With the help of sophisticated instrument, the hygroscopic characteristics of aerosols can be accurately measured for a specific area, yet these measurements are only available for limited regions worldwide (Hand and Malm, 2007). Particularly in vast developing countries like China, most hygroscopic studies are conducted in several megacities or populated regions and usually for a short period (Liu et al., 2008; X. Liu et al., 2009; Xu et al., 2002), which are insufficient for the regional or nationwide estimation of PM by satellites.

This paper presents a new empirical method of RH correction for the satellite estimation of surface PM. The local aerosol hygroscopicity is roughly characterized by the variations of aerosol average mass extinction efficiency with ambient RH, which are obtained from in-situ observations of visibility (VIS), RH and PM concentration. Benefiting from its observational basis, this method no longer depends on a priori information of aerosol chemical and microphysical properties, and achieves accurate RH correction for any regions where the in-situ measurements of VIS, RH and PM are available. It can further retrieve PM concentration from the satellite derived b_{ext} when assuming that the errors caused by AOD vertical correction are negligible. Moreover, this method is adaptive to the temporal variations of pollution emissions and meteorological conditions by updating the information of aerosol hygroscopicity every season or even every month, as long as the corresponding in-situ measurements are continuous and cover a long term.

The data processing and method description of this paper are introduced in Section 2. The results of hygroscopic model fitting and the performance of RH correction are given in Section 3. The validation of PM retrieval and the inspection of the effectiveness on satellite AOD of this method are also presented in Section 3. The conclusions and uncertainty analysis are given in Section 4.

2. Method and data

2.1. RH correction based on hygroscopic models

According to the Mie theory, the physical correlation between b_{ext} and PM could be expressed as below (Wang et al., 2010):

$$b_{ext} = \frac{3\langle Q_{ext}\rangle}{4r_{eff}\rho}\mathrm{PM} \tag{1}$$

Similar with the definition of the average mass scattering efficiency given by Hand and Malm (2007), we define the average mass extinction efficiency (α_{ext}) for an aerosol population as the ratio of b_{ext} to the mass concentration (e.g. PM) of that population. Obviously, α_{ext} only represents the average conditions of mixed aerosol samples, while their physical properties and compositions may be changing during the sampling period. Based on Eq. (1), α_{ext} can be written as:

$$\alpha_{ext} = \frac{b_{ext}}{\mathrm{PM}} = \frac{3\langle Q_{ext}\rangle}{4r_{eff}\rho} \tag{2}$$

$\langle Q_{ext}\rangle$ is the size-distribution integrated extinction efficiency. It depends on the aerosol composition and size distribution (Liou, 2004), both of which are highly associated with RH. r_{eff} and ρ are the effective radius and average mass density of the aerosols, respectively, and they are also correlated with RH (Tang, 1996; Liu, 2008). According to the review of Hand and Malm (2007), much of the variability of α_{ext} estimated using measurement method could be related to RH. When assuming that the chemical composition and size distribution of aerosols would change little during a certain period (Liu, 2008), α_{ext} can be approximately considered as a function of ambient RH, e.g. α_{ext} (RH).

Previous studies in aerosol hygroscopicity have shown that, the f(RH) of aerosol scattering (the ratio of aerosol scattering coefficient at ambient RH to that under dry conditions, e.g. RH $\leq$ 40%) could be well fitted by several non-linear models (Kotchenruther et al., 1999; Carrico et al., 2003; Liu et al., 2008). Considering that the hygroscopic effect on the aerosol absorption coefficient is insignificant (Nessler et al., 2005), and that the aerosol scattering and extinction coefficients usually have good correlations (Lee and Sequeira, 2001), those models used to fit the f(RH) of aerosol scattering (Kotchenruther et al., 1999) are modified through linear transformation to account for the difference between aerosol scattering and extinction, and will be used to fit the empirical functions of α_{ext} (RH) as below:

$$\text{Model 1}: \alpha_{ext}(\mathrm{RH}) = m\left(1-\frac{\mathrm{RH}}{100}\right)^{-g}+n \tag{3}$$

$$\text{Model 2}: \alpha_{ext}(\mathrm{RH}) = a\left(\frac{\mathrm{RH}}{100}\right)^{b}+c \tag{4}$$

$$\begin{aligned}\text{Model 3}: \alpha_{ext}(\mathrm{RH}) = {} & \left[a\left(\frac{\mathrm{RH}}{100}\right)^{b}+c\right]\left\{1-\frac{1}{\pi}\left\{\frac{\pi}{2}+\arctan\left[10^{24}\right.\right.\right.\\ & \left.\left.\left.\times\left(\frac{\mathrm{RH}}{100}-\frac{d}{100}\right)\right]\right\}\right\}+\left[m\left(1-\frac{\mathrm{RH}}{100}\right)^{-g}+n\right]\\ & \times\left\{\frac{1}{\pi}\left\{\frac{\pi}{2}+\arctan\left[10^{24}\left(\frac{\mathrm{RH}}{100}-\frac{d}{100}\right)\right]\right\}\right\}\end{aligned} \tag{5}$$

m, n, g, a, b, c and d are fitting coefficients for respective models, which are obtained from the observation datasets of α_{ext} and RH. The fitting performance of Model 1, 2 and 3 will be compared in Section 3.1, and only one of them will be used in further analysis and the final RH correction.

According to the definition of α_{ext}, the RH correction as well as PM retrieval can be simultaneously accomplished based on the fitted α_{ext} (RH):

$$PM = b_{ext}/\alpha_{ext}(RH) \quad (6)$$

2.2. Data description and processing

2.2.1. Ground-level data

2.2.1.1. Datasets from the supersite. To support the air quality protection during the Beijing 2008 Olympic Games and Paralympic Games, Chinese Academy of Sciences (CAS) implemented the Project of Ambient Air Monitoring in Beijing Area from August 2007 to September 2008, during which more than 20 observing stations have been set up in Beijing and its surrounding regions. One of the most comprehensive stations operated is the supersite (40.00N, 116.38E) on the roof of Institute of Remote Sensing Applications, CAS, which locates in the north of the urban area of Beijing (shown in Fig. 1). Nearly 20 instruments were installed to compose a complete air monitoring system. The concentrations of PM10 and PM2.5 are obtained by the Thermo RP 1400a Tapered Element Oscillating Microbalance (TEOM) (http://www.thermoscientific.com/en/home.html), which has an accuracy of ±1.5 μg/m^3 for 1 h average. VIS was measured by a forward scattering visibility-meter (http://www.ldchina.cn/NNews.asp?id=81), of which the measurement error ranges from ±10% (VIS ≤ 10 km) to ±20% (VIS > 20 km) (Li and Sun, 2009). RH was acquired by an automatic meteorological instrument, which also provides temperature, pressure, wind speed and directions at surface.

All the measurements of VIS, RH and PM10 are examined for data quality. Considering that the supersite is located at roadside and is very close to the National Stadium and Gymnasium for 2008 Olympic Games, the PM10 measurement may have abrupt increase during a short term, which is mainly caused by the active traffic emissions and construction dust nearby. Moreover, the high humidity in ambient air right after precipitation usually leads to very tiny or even negative PM10 concentrations. Therefore, the largest 5% of PM10 measurements of each month and those below 20 μg/m^3, as well as the data obtained during the precipitation are all excluded in this study. The hourly mean values of PM10, VIS and RH are matched to each other for α_{ext} calculation and further analysis. Due to a severe power cut and some instrumental anomalies lasting from late 2007 to March 2008, the observations in February are missing, and those in January and March are also incomplete. Consequently, the datasets of the three months, which takes up about 8.4% of the whole data samples, are not included in the fitting of α_{ext}–RH correlation.

The temporal variations of daily-averaged PM10, RH and VIS from September 2007 to August 2008 are presented in a sequence of Julian days in Fig. 2. Despite the missing data from late January to early March, VIS shows a reversed linear correlation with RH and PM10. All of these parameters have a relatively stable level from July to August (Julian Day 190–240), while much larger day-to-day fluctuations are found in the rest of year. The seasonal statistical summaries of PM10, RH and VIS are given in Table 1. Among all the seasons, winter has the highest PM10 concentrations (218.3 μg/m^3) while summer has the lowest ones (143.1 μg/m^3). The highest RH (61.8%) and VIS (19.2 km) are both found in summer, while the lowest RH (47.8%) occurs in winter and the lowest VIS (12.7 km) is found in fall.

This study used VIS measured by a forward scattering visibility-meter to derive b_{ext}. Unlike a transmission-meter that directly acquires the average extinction through a certain length of atmosphere, visibility-meter measures the forward scattering of ambient air and converts it into VIS. The conversion relies on a series of assumptions, such as a constant scattering phase function, constant single scattering albedo (SSA), and negligible absorption. Consequently, the measured visibility may have considerable uncertainty due to the variation of aerosol compositions and size distributions, as well as the ambient humidity. Depending on different types of aerosols, namely fog, rural or urban, the

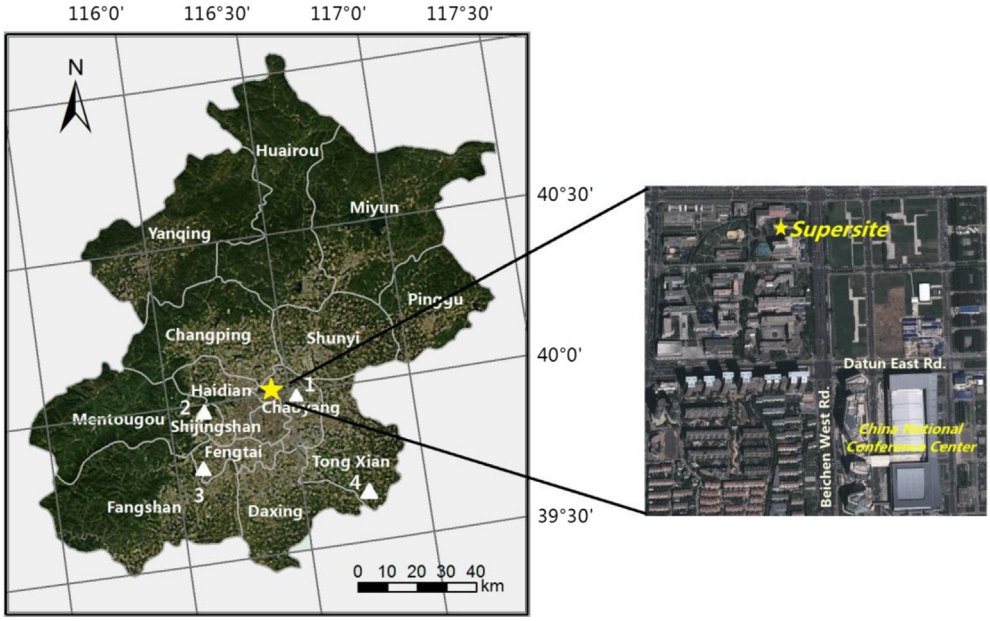

Fig. 1. Terrain of Beijing and the locations of the supersite (yellow pentacle) and the four validation sites (red triangles: 1-Bj-tower, 2-Shougang, 3-Yungangzhen, 4-Yongledian). (For interpretation of the references to color in this figure legend, the reader is referred to the web version of this article.)

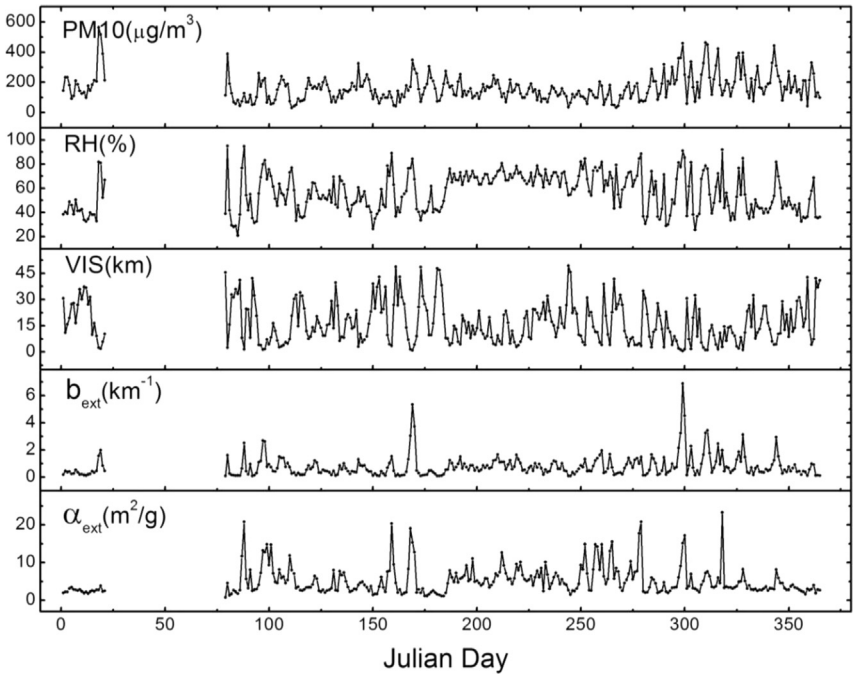

Fig. 2. Temporal variations of daily averaged PM10, VIS, RH, b_{ext} and α_{ext} measured at the supersite in Beijing from September 2007 to August 2008. The dataset from the late January to the middle March (Julian day 22–78) are missing due to a power cut and instrument anomalies.

maximum error of measured VIS ranges from 7% to 18% (Li and Sun, 2009). Based on the empirical correlation given by Koschmieder (1925), the total atmospheric extinction coefficient ($b_{ext,atm}$) is derived from VIS by using $b_{ext,atm} = 3.912/VIS$. It should be noted that, the Koschmieder formula is applicable under very limited conditions: the atmosphere must be illuminated homogeneously, the extinction coefficient and the scattering function do not vary with space, and there must be an ideally black object and a constant contras threshold (Horvath, 1971). Hence using the formula may also induce some uncertainty into the calculation of $b_{ext,atm}$, and then affect the accuracy of b_{ext}. By removing the contribution of molecular scattering ($b_{sca,m}$) and absorption ($b_{abs,m}$) from $b_{ext,atm}$, b_{ext} is computed as below:

$$b_{ext} = 3.912/VIS - b_{sca,m} - b_{abs,m} \quad (7)$$

According to Xu (2005), $b_{sca,m} = 32\pi^3/3\lambda^4 \cdot (n-1)^2/N$, where n is the atmospheric refractive index of ($n - 1 = 293^{*}10^{-6}$ at the sea level), and N stands for the volume number density of molecules ($N = 266^{*}10^{19}$ cm^{-3} at the sea level). $b_{abs,m}$ is approximately represented by NO_2 absorption in Beijing area (Liu, 2008), which is calculated based on ground-level NO_2 concentration as $b_{abs,m} = 3.3 \cdot C_{NO_2}$ (Hodkinson, 1966). C_{NO_2} is the NO_2 concentration in ppmv, which is also one of the primary pollutants measured in most of the air quality monitoring sites in China. During the CARE-Beijing field campaign from August to September, 2006, Jung et al. (2009) obtained an average ambient air extinction coefficient of 0.88 ± 0.67 km^{-1} using a transmission-meter. In the same campaign, Liu (2008) calculated b_{ext} as the total of the observed aerosol scattering coefficient and absorption coefficient under ambient conditions, which is 0.77 ± 0.79 km^{-1}. The seasonal average of b_{ext} in summer in this paper (0.66 ± 0.94 km^{-1}) is close to the results of these previous studies.

Based on the computed b_{ext} and PM10 concentration, α_{ext} is calculated using Eq. (2). Both of b_{ext} and α_{ext} are calculated at 0.55 μm, being consistent with satellite AOD retrievals. The temporal variations of daily-averaged b_{ext} and α_{ext} are also plotted in Fig. 2, and their basic statistic summaries are given in Table 1.

2.2.1.2. Datasets from the other sites. In order to validate the performance of the new RH correction method on satellite data, more in-situ measurements of PM10 over a large area are needed. Since the empirical α_{ext} (RH) is fitted based on the datasets from the supersite alone, its spatial representativeness may be limited due to

Table 1
Annual and seasonal statistical summaries of hourly PM10 concentrations, RH, VIS, as well as b_{ext} and α_{ext} from the whole dataset from September 2007 to August 2008.

Season	Variable	Mean±	SD[a]
Annual $N = 7554$	PM10 (μg/m^3)	171.1	119.9
	VIS (km)	16.0	15.2
	RH (%)	54.8	20.3
	b_{ext} (km^{-1})	0.74	0.98
	α_{ext} (m^2/g)	4.43	5.21
Spring $N = 1770$	PM10 (μg/m^3)	154.6	87.7
	VIS (km)	15.2	13.8
	RH (%)	50.1	19.6
	b_{ext} (km^{-1})	0.59	0.57
	α_{ext} (m^2/g)	4.02	3.71
Summer $N = 1988$	PM10 (μg/m^3)	143.1	90.2
	VIS (km)	19.2	17.1
	RH (%)	61.8	17.9
	b_{ext} (km^{-1})	0.66	0.94
	α_{ext} (m^2/g)	4.71	5.74
Fall $N = 2105$	PM10 (μg/m^3)	185.0	130.9
	VIS (km)	12.7	13.8
	RH (%)	59.1	21.7
	b_{ext} (km^{-1})	1.05	1.29
	α_{ext} (m^2/g)	5.67	6.63
Winter[b] $N = 1072$	PM10 (μg/m^3)	218.3	147.7
	VIS (km)	15.1	14.9
	RH (%)	47.8	16.8
	b_{ext} (km^{-1})	0.73	0.97
	α_{ext} (m^2/g)	3.08	2.37

[a] Standard deviation.
[b] The winter dataset only consists of measurements in December.

spatial variations of aerosol physical and chemical properties. Hence only four observing sites in Beijing other than the supersite are selected for the validation of satellite retrieval of PM. However, the PM10 measurements in the four sites are only available from late July to August, 2008, which greatly limited the sample size of validation data after matching PM10 with the satellite and model data. The locations of the four validation sites, namely 1) Bj-tower, 2) Shougang, 3) Yungangzhen and 4) Yongledian, are marked by the triangles with corresponding numbers in Fig. 1, and their distances from the supersite are 4 km, 20 km, 30 km and 50 km, respectively. Among the four sites, Bj-tower and Shougang are located at urban areas, while Yungangzhen and Yongledian are located at suburban and rural areas, respectively.

2.2.2. Satellite data

To further validate the new method's applicability on satellite retrieval of surface PM, the AOD product of Moderate Resolution Imaging Spectroradiometer (MODIS) onboard NASA Terra satellite are employed. The retrieving process of MODIS AOD over land is only performed during daytime and for the cloud-free and dark pixels. The Level 2 AOD is retrieved at a resolution of 10*10 km at nadir through a procedure that includes the discrimination of cloud, selection of dark pixels, and determination of aerosol model (Remer et al., 2006). An extensive effort of validation using over 8000 MODIS retrievals collocated with AERONET AOD measurement indicates that globally, the MODIS products have an accuracy of $\pm 0.05 \pm 0.15\tau$ over land and $\pm 0.03 \pm 0.05\tau$ over ocean (Remer et al., 2005). The one-hour averages of the PM10 obtained during the satellite's overpassing time from each validation site are matched with the MODIS Level 2 AOD pixels covering the corresponding site.

2.2.3. Model simulation

When retrieving surface PM from MODIS AOD, the measurements of aerosol vertical profiles are currently not available over large regions, and thus the simulation results from chemical transport models are needed to fill in this information. In this study, a regional air quality model RAMS-CMAQ was chosen to simulate the aerosol profiles as well as RH in Beijing area, and the detailed descriptions and performance of this model can be found in the work of Han et al. (2011). The simulation has 94 × 90 grid cells with a resolution of 16 km, which are centered at Beijing (116°E, 40°N) and cover most parts of the North China Plain (NCP). The model system has 15 vertical layers, unequally spaced from the ground to approximately 23 km, with nearly half of them concentrated in the lowest 2 km to improve the simulation of the atmospheric boundary layer. The time step of the simulation is 1 h. According to Han et al. (2013), the RAMS-CMAQ model well captured the spatial and temporal variations of PM concentration in NCP. The MODIS AOD is matched with the simulated aerosol profiles and RH from the nearest model grid according to the overpass time of the satellite.

3. Result and discussion

3.1. α_{ext} (RH) fitting

Fig. 3 presents the scatterplots of hourly-averaged α_{ext} versus RH for the entire datasets in all the four seasons. In general, the humidographs in summer and fall both have nearly flat growths at medium RH (40%–80%) and sharp increases at high RH (>80%), indicating a mixture of two categories of aerosol growth with RH, namely deliquescent and hygroscopic (Kotchenruther et al., 1999). On the other hand, both of the humidographs in spring and winter have relatively low increases of α_{ext} at high RH (>80%). While an overall hygroscopic growth is dominant and no obvious deliquescence point exists in spring, it shows an obvious deliquescent behavior in the humidograph in winter. It should be noted that the winter dataset only includes December data, thus the observation statistics as well as the α_{ext}–RH association might be less representative than those of other seasons. The distinct variation trends of α_{ext} with RH among summer-fall, spring and winter indicate the seasonal differences in chemical compositions and source contributions of aerosols in Beijing (Zheng et al., 2005).

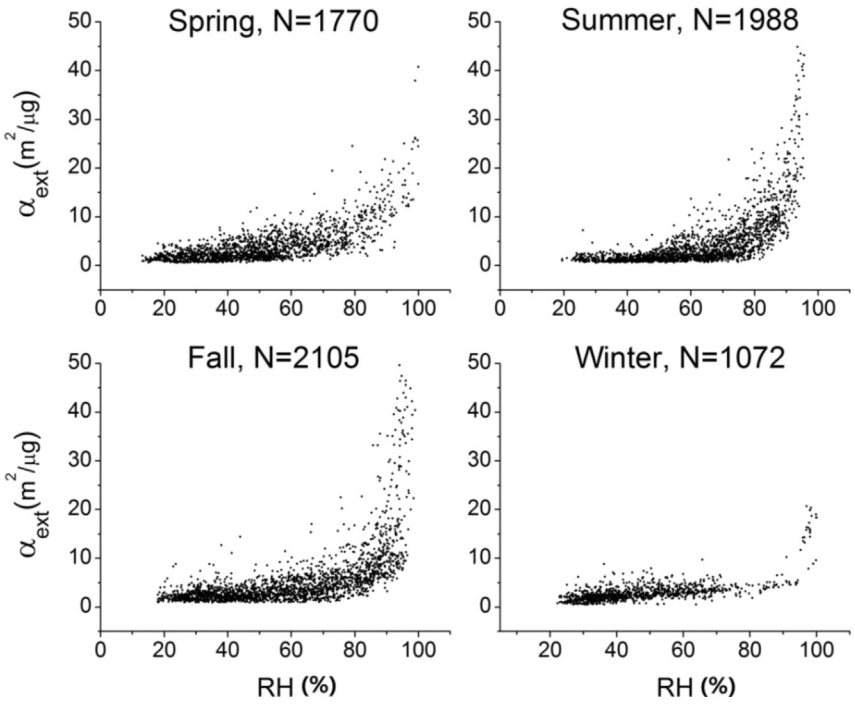

Fig. 3. Seasonal scatterplots of hourly-averaged α_{ext} versus RH for the datasets of the entire day.

Table 2
Annual and seasonal statistical summaries of hourly α_{ext} and RH from the extracted datasets within the daytime section covering the satellite overpass time.

Season	Variable	Mean	SD
Annual $N = 2525$	α_{ext} (m^2/g)	3.90	4.51
	RH (%)	45.6	18.2
Spring $N = 569$	α_{ext} (m^2/g)	3.55	3.00
	RH (%)	40.5	15.8
Summer $N = 702$	α_{ext} (m^2/g)	4.33	5.30
	RH (%)	54.3	17.4
Fall $N = 821$	α_{ext} (m^2/g)	4.7	5.6
	RH (%)	49.8	20.0
Winter $N = 433$	α_{ext} (m^2/g)	2.92	2.56
	RH (%)	42.7	17.2

It should be mentioned that, b_{ext} derived from VIS in this study has no particle size cut. If the particles larger than PM10 contributes a lot to the total aerosol extinction, e.g. when dust transport occurring, the calculated α_{ext} would be larger than it actually was. In addition, when using TEOM to measure PM10, the required heating on the sampled air may cause some loss of semi-volatile aerosol components, which makes the measured PM10 concentrations lower than those in ambient air, and may lead to as high as fourfold difference between the theoretical and the calculated α_{ext} (Bergin et al., 2001). Both of these uncertainties could lead to α_{ext} overestimation at any RH level, which may explain some of the high values of α_{ext} at low or medium RH in Fig. 3.

Since the main interest of this study is the RH correction on satellite AOD, only the datasets within the section of daytime that covers the overpass time of most earth-observing satellites, namely 9:00–16:00 local time, are extracted for the α_{ext} (RH) fitting. The extracted datasets take up nearly 34% of data samples of the whole datasets. Table 2 presents the annual and seasonal statistics of the extracted α_{ext} and RH. Fig. 4 shows the scatterplots of the extracted datasets for each season. Compared to summer and fall, fewer data samples of high RH (>80%) remain in the extracted datasets in spring and winter. The regressions of Model 1, 2 and 3 (e.g. Eqs. (7)–(9)) in Section 2.1 are conducted respectively on the extracted datasets for each season, and the fitting curves are also plotted in Fig. 4. Those curves of the three models are quite similar in summer, fall and winter, while in spring the fitting curve of Model 2 is distinct from those of Model 1 and Model 3 when RH is over 70%. Among the three curves, Model 1 and Mode 3 are relatively closer to each other in all seasons except fall, in which Model 2 and Model 3 are a bit more alike. According to the R^2 of the fitting curves, Model 3 has overall the best fitting performance on the whole datasets. Model 1 is very close to Model 3 in all seasons, while Model 2 does not perform well in spring. In order to obtain a simple and consistent RH correction method, Model 1 is chosen for further α_{ext} (RH) fitting.

To achieve more accurate RH correction, Model 1 is fitted specifically on each of the nine months with sufficient (e.g. no less than 150) data samples. Fig. 5 shows the fitting results of all the nine available months. As one can see, the fitting performance is much better on monthly basis than that on seasonal basis. The mean value of correlation R^2 of the nine fitting curves is 0.71, and six of them have a R^2 above 0.73. The regression coefficients of Model 1 for each of the nine months are given in Table 3. The differences of these coefficients among different months indicate that, the monthly variations of aerosol chemical compositions and size distributions are not negligible. On the other hand, there are still several outliers (data spots far from the fitting curve) in each humidographs in Fig. 5, which imply that the fitted model can only represent an average variation trend of α_{ext} with RH, and thus uncertainties may remain in the further RH correction on b_{ext} and the retrieval of PM10.

3.2. RH correction on b_{ext}

Once the fitted α_{ext} (RH) are obtained in Section 3.1, RH correction is conducted on b_{ext} for each of the nine available months based on Eq. (6), through which the retrieval of PM10 is implemented simultaneously. Both of the scatterplots of the observed PM10 with b_{ext} and those of the observed PM10 with the

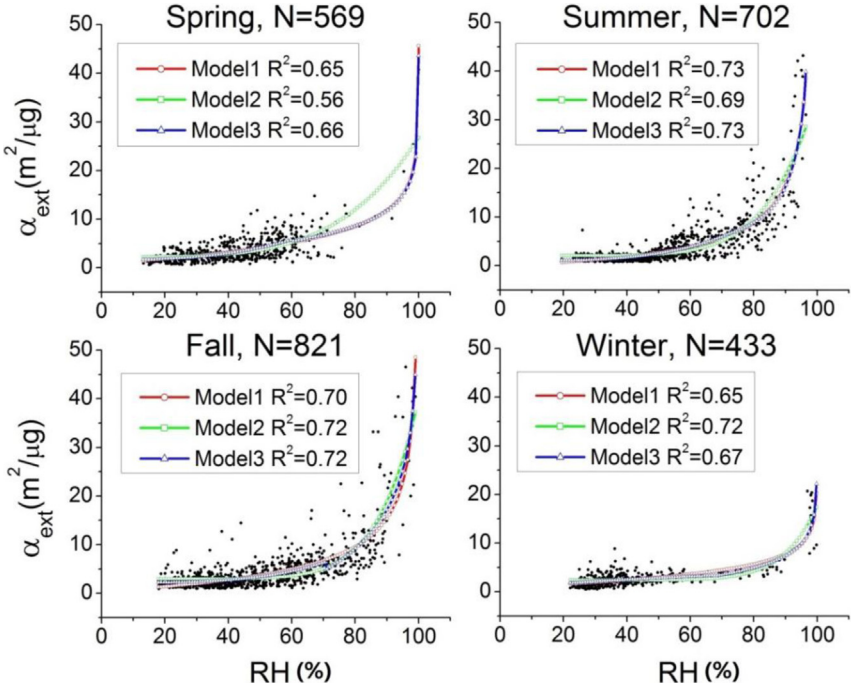

Fig. 4. Same as Fig. 3 but for the datasets within the section of daytime covering the satellite overpass time, as well as the fitting curves of the three empirical models.

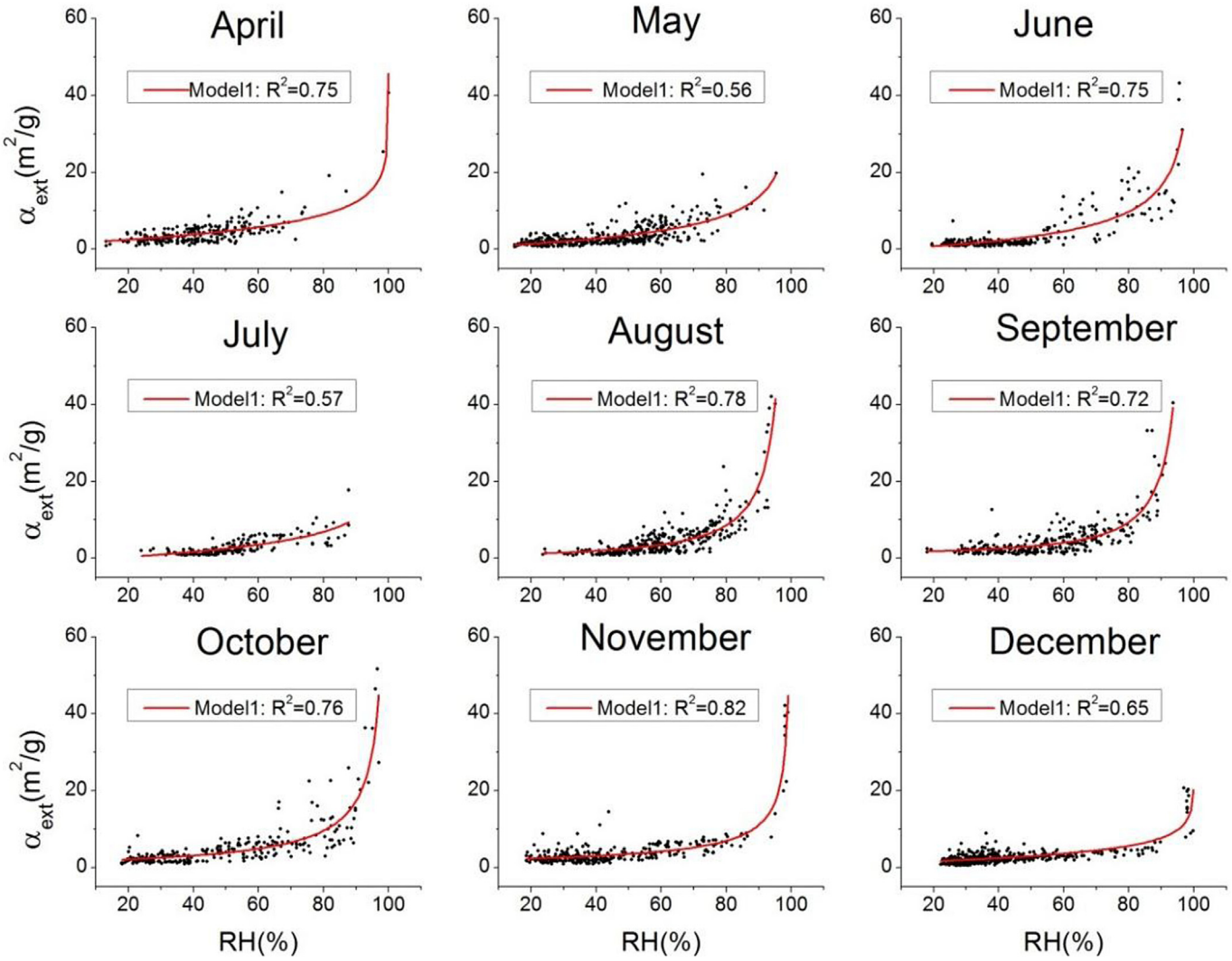

Fig. 5. Scatterplots between α_{ext} versus RH, as well as the fitting curves of Model 1 for each of the nine months with sufficient data samples.

retrieved PM10 are given in Fig. 6. As one can see, the b_{ext}–PM10 correlations in all these months are greatly improved by RH correction, particularly in May, June, August and December. Moreover, the correlation of the retrieved and the observed PM10 for the whole year's dataset increases substantially compared to that of b_{ext} and the observed PM10, which also illustrates the effectiveness of RH correction during a relative long term.

The double cross-validation method is used to evaluate the performance of this RH correction and PM10 retrieving method. In order to have enough data samples for the model training and validation, the seasonal datasets are used instead of the monthly ones. Each of the seasonal datasets is randomly divided into two approximately equal subsets, namely the modeling and validation groups, which have similar probability distributions for all the parameters. The α_{ext} (RH) is fitted on the modeling datasets for each season, and is then used to conduct RH correction and PM10 retrieval for both of the modeling and validation datasets. The comparisons between the retrieved and the observed PM10 concentrations for both datasets in all the four seasons are shown in Fig. 7, and their good agreement indicates the effectiveness of RH correction method in retrieving PM concentration from aerosol extinction coefficient. Among all the seasons, fall has the highest R^2 of 0.73, while spring has the lowest one of 0.54. The mean relative discrepancies between the retrieved and observed PM10 concentrations in validation datasets are −2.5% in winter, −4.7% in fall, −9.4% in summer, and −10.8% in spring.

On the other hand, considerable uncertainties still remain between the retrieved and the observed PM10, which can be partially attributed to the b_{ext} derivation from visibility-meter and the PM10 measurement, as stated in Section 2.2 and 3.1. In addition, the fitting of α_{ext} (RH) may also bring errors into the retrieval of PM10. There are too few data points for high RH (e.g. >80%), at which α_{ext} becomes very sensitive to RH. The shape of the fitting curve at high RH is determined by very limited points and thus has considerable uncertainty. Further comparisons under different RH levels show that, the α_{ext} (RH) fitted based on Model 1 tend to underestimate PM10 at low and medium RH (e.g. <60%) but to overestimate PM10 at high RH (e.g. >60%). Given that most of the data records are obtained at low and medium RH, this error may partially explain the general minus biases of the retrieved PM10 against the observed ones in Fig. 7. Using the other two models instead of Model 1 has similar results.

3.3. Application on satellite retrieval of PM

The new RH correction method is further applied on satellite data to examine its performance in improving the retrieval of surface PM10. According to method presented by X. Liu et al.

Table 3
Regression coefficients of Model 1 fitted for each of the nine months with sufficient data samples.

Coefficient	April	May	June	July	August	September	October	November	December
g	0.002245	0.2117	0.3904	0.127	1.05	1.268	0.7323	0.5629	0.01121
m	2.112	0.02111	0.01158	0.02553	0.0018	0.001199	0.003611	0.003472	0.2356
n	−2.111	−0.02078	−0.01191	−0.02525	−0.001152	0.000218	−0.002152	−0.001623	−0.2345

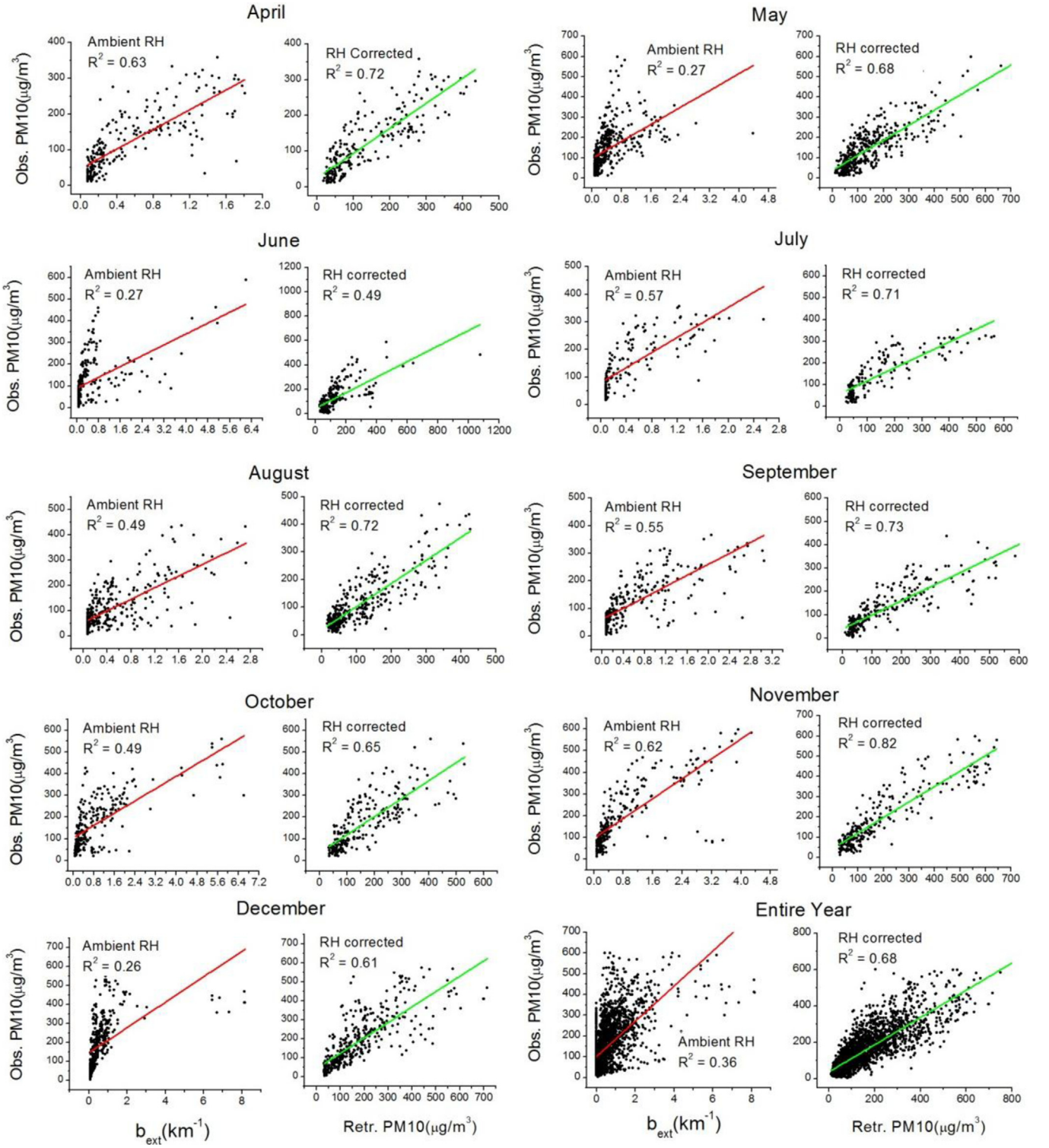

Fig. 6. Scatterplots of the observed (Obs.) PM10 and b_{ext} (with a red solid fitting line) and those of the Obs. PM10 and the retrieved (Retr.) PM10 (with a green solid fitting line) for each of the nine months with sufficient data samples, as well as for the whole year's dataset. (For interpretation of the references to color in this figure legend, the reader is referred to the web version of this article.)

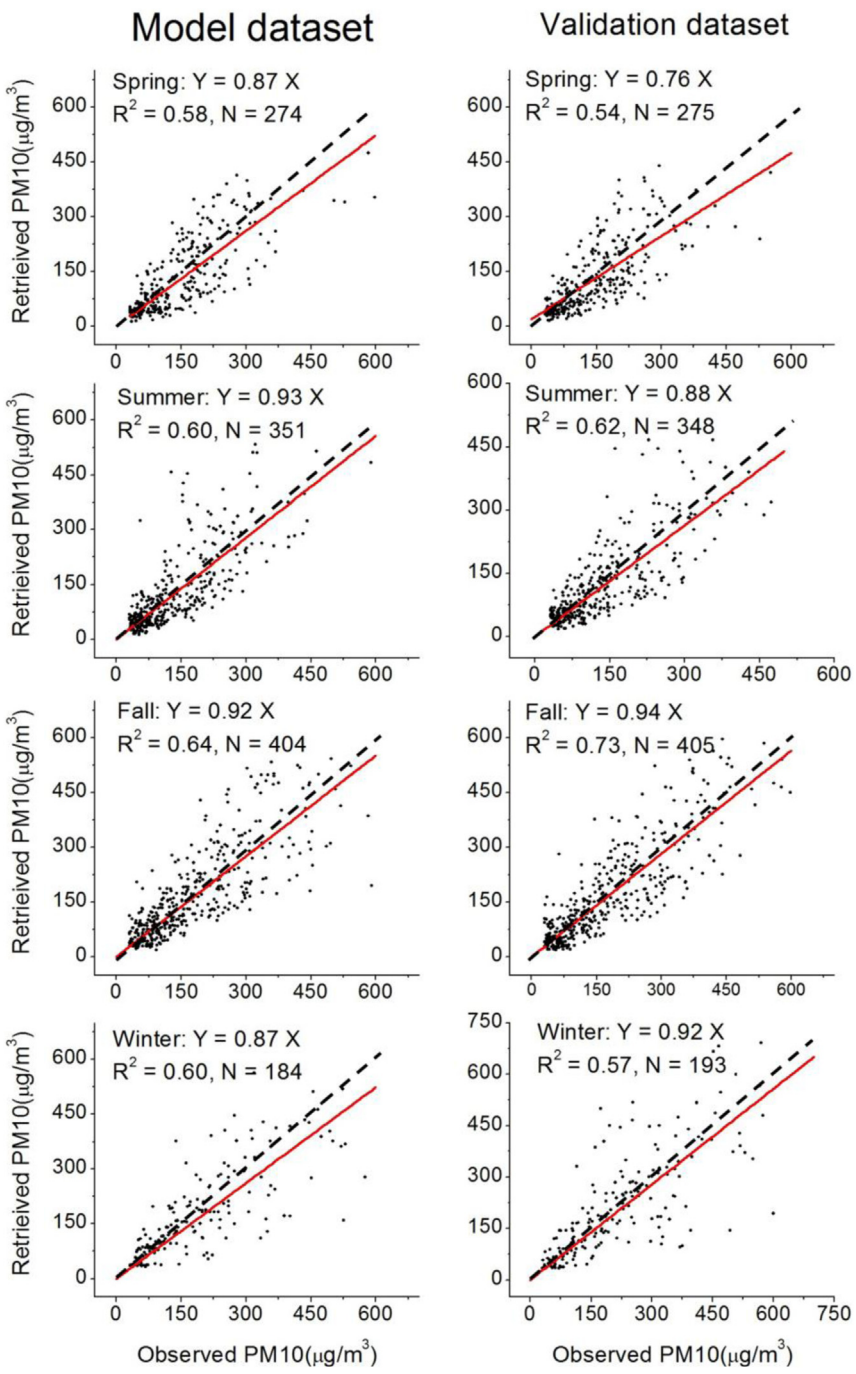

Fig. 7. Comparisons between the retrieved and the observed PM10 concentrations for the modeling (left) and the validation (right) datasets, respectively, in all the four seasons. The fitting lines (red solid) and the Y = X lines (black dashed) are also plotted. (For interpretation of the references to color in this figure legend, the reader is referred to the web version of this article.)

(2009), Y. Liu et al. (2009), the simulated aerosol profiles from RMAS-CMAQ are used to extract the aerosol extinction near surface. We define the bottom aerosol proportion as the ratio of the simulated PM10 concentration within the lowest 4 layers (on average 0.5 km above the ground) to the total PM10 concentration. These proportions are used to scale the satellite columnar AOD, and the b_{ext} is further estimated from the scaled AOD by assuming a well-mixed aerosol mass under the height of the 4th layer (H_{low}).

$$b_{ext} = \mathrm{AOD}_{column} \cdot \frac{\mathrm{PM10}_{low}}{\mathrm{PM10}_{total}} \cdot \frac{1}{H_{low}} \quad (8)$$

The model simulated RH is used to calculate α_{ext} (RH) and then the retrieved PM10 concentration is obtained by applying Eq. (6) on the satellite derived b_{ext}.

The retrieved PM10 and the measured ones from the corresponding validation sites are compared in Fig. 8, in which comparisons of the measured PM10 with satellite AOD and the derived b_{ext} are also plotted. Compared to the poor correlation between AOD and PM10 ($R^2 = 0.19$), a better correlation between b_{ext} and PM10 is achieved by the vertical correction based on the simulated aerosol profiles ($R^2 = 0.29$). After the RH correction, the R^2 between the retrieved PM10 and the measured ones is further improved to

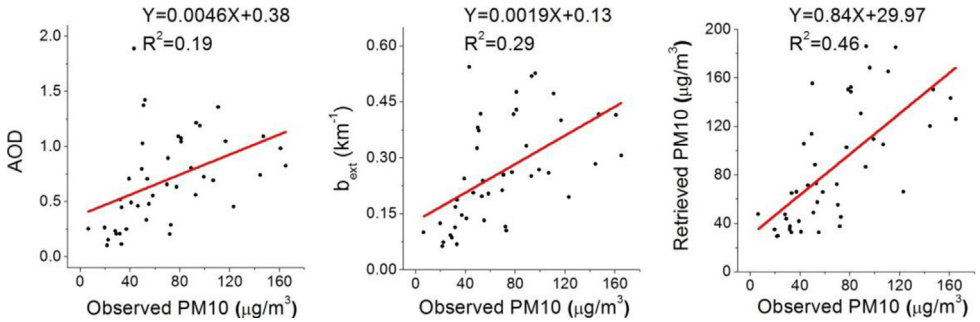

Fig. 8. Scatterplots of AOD (left), b_{ext} (middle) and PM10 (right) retrieved from MODIS data with the PM10 measured from the four validation sites in Beijing from late July to August, 2008 ($N = 44$).

0.46, and the relative retrieving error is 19.3%. By comparing the b_{ext} derived from satellite and that observed by visibility-meter at the supersite, we found that the satellite b_{ext} is larger than the observed one by 31.6% on average, which may partially contributed to the satellite overestimation of surface PM10. Although there still exist uncertainties between the observed and the retrieved PM10, which can be attributed to the accuracy of AOD retrieval, model simulation, the effectiveness of the vertical correction on AOD, as well as the spatial representativeness of α_{ext} (RH), the results demonstrates the good potential of this new method of RH correction in improving the satellite retrieval of surface PM.

To date, there are over 700 meteorological sites (China Meteorological Data Sharing Service System, http://cdc.cma.gov.cn/home.do) and more than 500 air quality monitoring sites (Ministry of Environmental Protection, http://113.108.142.147:20035/emcpublish/) are in operation across mainland China. Most of the air quality monitoring sites are close to one or more meteorological sites, and the collocated measurements of VIS, RH and PM allow this new method to be easily applied to other regions with similar performances. These nationwide observation networks provide an unprecedented opportunity to extend the spatial and temporal coverage of accurate RH correction, so as to improve the satellite estimation of PM in China. Although $PM_{2.5}$ observations have been available in over 70 cities in China since January, 2013, the monitoring networks of PM10 have larger spatial coverage and their data records are much longer compared to PM2.5. Therefore, this study chose to use PM10 in the development and analysis of the new method for better applicability in China.

4. Conclusion

This study develops an empirical RH correction method for the second step, so as to improve the correlation between b_{ext} and surface PM concentration. When assuming the composition and size distribution of aerosols change little during a certain period, α_{ext}, defined as ratio of b_{ext} to the mass concentration of these aerosols, is approximately considered as a function of RH. Several non-linear models, which are adapted from empirical models that characterize the hygroscopic growth behaviors of aerosol scattering, are employed to fit α_{ext} based on in-situ measurements. The fitted α_{ext} (RH) would be used to conduct RH correction on b_{ext}, and to further retrieve PM10 concentration. Nearly one-year of in-situ measurements of PM10 concentration, VIS and RH collected in Beijing urban area are used for the model fitting of α_{ext} (RH). The distinct scatterplots of α_{ext}–RH in different seasons clearly indicate the seasonal variations of aerosol compositions and size distributions. In order to make RH correction more specific for satellite retrieval of PM, only the datasets within the daytime section covering satellite overpass time are extracted for α_{ext} (RH) fitting, and a simple power function is selected as the empirical model. The α_{ext} (RH) fitting is implemented on each of the nine months with sufficient data samples, and good fitting performances are achieved with an average correlation R^2 of 0.71.

Through RH correction, the correlation between b_{ext} and PM10 is significantly improved in each of the nine months, and the correlation R^2 of the whole year's dataset increases from 0.36 to 0.68. According to the definition of α_{ext}, the RH correction and the PM10 retrieval can be achieved simultaneously. To validate the performance of PM10 retrieval, the dataset of each season is randomly divided into two independent and nearly equal subsets, namely the modeling and the validation groups. The regression coefficients of the fitted α_{ext} (RH) are obtained from the modeling groups, and then applied on the validation groups to retrieve PM10 concentrations. Good agreements between the retrieved and the observed PM10 are achieved in all the four seasons, with R^2 ranging from 0.54 to 0.73 and the relative errors ranging from −2.5% to −10.8%. To further examine the method's effectiveness on satellite retrieval of surface PM, MODIS AOD and RAMS-CMAQ simulated aerosol profiles are used to derive the regional b_{ext} in Beijing. Then regional PM10 is retrieved through the RH correction on the satellite derived b_{ext}. Only the PM10 measurements from four observing sites other than the supersite in Beijing are selected for validation. The correlation between the retrieved and the observed PM10 ($R^2 = 0.46$) is greatly improved from that between satellite AOD and the observed PM10 ($R^2 = 0.19$), and the retrieving error is 19.3%. Considerable uncertainties still remain in the PM10 retrievals, most of which may stem from satellite AOD retrieval, model simulation, vertical correction on AOD, as well as the new RH correction methods.

Although the initial validations have indicate the great potential of the new RH correction method in improving the satellite retrieval of surface PM, more in-situ data are needed for further validations at larger spatial and temporal scales, so as to fully evaluate the method's performance. Moreover, the uncertainties induced by the calculation of b_{ext} from VIS observations, as well as the validity of the assumption of nearly constant aerosol composition and size distribution must be carefully considered when using this method. In future studies, the particle sources provided by backward trajectory models as well as the aerosol size distributions retrieved from in-situ measurements would be introduced to this method, which are expected to further improve the accuracy of RH correction.

Acknowledgements

This study was funded by National Natural Science Foundation of China (Grant No. 41201333) and the Type B Strategic Pilot Special Project of Chinese Academy of Sciences (XDB05030100). We thank

Doctor Jianguo Liu from Anhui Institute of Optics and Fine Mechanism, CAS for his help in the instrument maintenance and data processing. We are grateful to Dr Xiao Han from Institute of Atmospheric Physics, CAS for his offering of RAMS-CMAQ simulations. The authors also appreciate Dr. Lin Su, Dr. Xiaoying Li, Dr. Shenshen Li, Dr. Ying Zhang, Dr. Mingmin Zou, and Chao Yu for their suggestions and help.

References

Bergin, M., Cass, G., Xu, J., Fang, C., Zeng, L., Yu, T., Salmon, L., Kiang, C., Tang, X., Zhang, Y., Chameides, W., 2001. Aerosol radiative, physical, and chemical properties in Beijing during 1999. J. Geophys. Res. 106, 17969–17980.

Carrico, C.M., Kus, P., Rood, M.J., Quinn, P.K., Bates, T.S., 2003. Mixtures of pollution, dust, sea salt, and volcanic aerosol during ACE-Asia: radiative properties as a function of relative humidity. J. Geophys. Res. 108 http://dx.doi.org/10.1029/2003JD003405.

Donkelaar, A.V., Martin, R.V., Park, R.J., 2006. Estimating ground-level PM2.5 using aerosol optical depth determined from satellite remote sensing. J. Geophys. Res. 111 (D21201), 1–10.

Guo, J., Zhang, X., Che, H., Gong, S., et al., 2009. Correlation between PM concentrations and aerosol optical depth in eastern China. Atmos. Environ. 43, 5876–5886.

Han, X., Zhang, M., Han, Z., Xin, J., Liu, X., 2011. Simulation of aerosol direct radiative forcing with RAMS-CMAQ in East Asia. Atmos. Environ., 6576–6592.

Han, X., Zhang, M., Tao, J., Wang, L., Gao, J., Wang, S., Chai, F., 2013. Modeling aerosol impacts on atmospheric visibility in Beijing with RAMS-CMAQ. Atmos. Environ., 177–191.

Hand, J.L., Malm, W.C., 2007. Review of aerosol mass scattering efficiencies from ground-based measurements since 1990. J. Geophys. Res. 112, D16203.

Hodkinson, R.J., 1966. Calculations of colour and visibility in urban atmospheres polluted by gaseous NO_2. Int. J. Air Water Pollut. 10, 137–144.

Hoff, R.M., Christopher, S.A., 2009. Remote sensing of particulate pollution from space: have we reached the promised land. J. Air Waste Manag. Assoc. 59, 645–675.

Horvath, H., 1971. On the applicability of the Koschmieder visibility formula. Atmos. Environ. 5, 177–184.

Hutchison, K.D., Faruqui, S.J., Smith, S., 2008. Improving correlations between MODIS aerosol optical thickness and ground-based PM2.5 observations through 3D spatial analyses. Atmos. Environ. 42, 530–543.

Jung, J., Lee, H., Kim, Y., Liu, X., Zhang, Y., Hu, M., Sugimoto, N., 2009. Optical properties of atmospheric aerosols obtained by in situ and remote measurements during 2006 Campaign of Air Quality Research in Beijing (CAREBeijing-2006). J. Geophys. Res. 114, D00G02 http://dx.doi.org/10.1029/2008JD010337.

Koelemeijer, R.B., Homan, C.D., Matthijsen, J., 2006. Comparison of spatial and temporal variations of aerosol optical thickness and particulate matter over Europe. Atmos. Environ. 40, 5304–5315.

Koschmieder, H., 1925. Theorie der horizontalen Sichtweite II: Kontrast und Sichtweite. Beiträge zur Physik der Freien Atmosphäre 12, 171–181.

Kotchenruther, R.A., Hobbs, P.V., Hegg, D.A., 1999. Humidification factors for atmospheric aerosols off the mid-Atlantic coast of the United States. J. Geophys. Res. 104, 2239–2251.

Lee, Y., Sequeira, R., 2001. Visibility degradations across Hong Kong: its components and their relative contributions. Atmos. Environ. 35, 5861–5872.

Li, H., Sun, X., 2009. Theoretical analysis on measurement error of forward scattering visibility meter. Infrared Laser Eng. 38, 1094–1098.

Li, C., Mao, T., Lau, A.K., Yuan, Z., Wang, M., Liu, X., 2005. Application of MODIS aerosol product in the study of air pollution in Beijing. Sci. China Ser. D Earth Sci. 35, 177–186.

Liou, K.N., 2004. An Introduction to Atmospheric Radiation (Chinese Translation), second ed. China Meteorological Press, Beijing, pp. 95–96.

Liu, X., 2008. Research on Aerosol Hygroscopic Properties by Measurement and Model: Taking Beijing and PRD Region for Examples (Doctoral dissertation). Peking University, Beijing.

Liu, Y., Sarnat, J.A., Kilaru, A., Jacob, D.J., Koutrakis, P., 2005. Estimating ground-level PM2.5 in the Eastern United States using satellite remote sensing. Environ. Sci. Technol. 39, 3269–3278.

Liu, X., Cheng, Y., Zhang, Y., Jung, J., Sugimoto, N., Chang, S., Kim, Y., Fan, S., Zeng, L., 2008. Influence of relative humidity and particle chemical composition on aerosol scattering properties during the 2006 PRD campaign. Atmos. Environ. 42, 1525–1536.

Liu, X., Zhang, Y., Jung, J., Gu, J., Li, Y., Guo, S., Chang, S., Yue, D., Lin, P., Kim, Y., Hu, M., Zeng, L., Zhu, T., 2009. Research on hygroscopic properties of aerosols by measurement and modeling during CAREBeijing-2006. J. Geophys. Res. 114, D00G16 http://dx.doi.org/10.1029/2008JD010805.

Liu, Y., Schichtel, B.A., Koutrakis, P., 2009. Estimating particle sulfate concentrations using MISR retrieved aerosol properties. IEEE J. Sel. Top. Appl. Earth Obs. Remote Sens. 2, 176–184.

Liu, Y., Wang, Z., Wang, J., Ferrare, R., Newsom, R., Welton, E., 2011. The effect of aerosol vertical profiles on satellite-estimated surface particle sulfate concentrations. Remote Sens. Environ. 115, 508–513.

Martin, R., 2008. Satellite remote sensing of surface air quality. Atmos. Environ. 42, 7823–7843.

Nessler, R., Weingartner, E., Baltensperger, U., 2005. Effect of humidity on aerosol light absorption and its implications for extinction and the single scattering albedo illustrated for a site in the lower free troposphere. J. Aerosol Sci. 36, 958–972.

Pelletier, B., Sater, R., Vidot, J., 2007. Retrieving of particulate matter from optical measurement: a semiparametric approach. J. Geophys. Res. 112, 1–18.

Remer, L.A., Kaufman, Y.J., Tanré, D., et al., 2005. The MODIS aerosol algorithm, products, and validation. J. Atmos. Sci. 62, 947–973.

Remer, L.A., Tanré, D., Kaufman, Y.J., Levy, R.C., Mattoo, S., 2006. Algorithm for Remote Sensing of Tropospheric Aerosol From MODIS: Collection 005. Algorithm Theoretical Basis Document.

Tang, I.N., 1996. Chemical and size effects of hygroscopic aerosols on light scattering coefficients. J. Geophys. Res. 101 (D14), 19245–19250.

Tian, J., Chen, D., 2010. A semi-empirical model for predicting hourly ground-level fine particulate matter (PM2.5) concentration in southern Ontario from satellite remote sensing and ground-based meteorological measurements. Remote Sens. Environ. 114, 221–229.

Wang, Z., Chen, L., Tao, J., Zhang, Y., Su, L., 2010. Satellite-based estimation of regional particulate matter (PM) in Beijing using vertical-and-RH correcting method. Remote Sens. Environ. 114, 50–63.

Xu, X., 2005. Remote Sensing Physics. Peking University Press, Beijing, pp. 331–332.

Xu, J., Bergin, M.H., Yu, X., Liu, G., et al., 2002. Measurement of aerosol chemical, physical and radiative properties in the Yangtze delta region of China. Atmos. Environ. 36, 161–173.

Zheng, M., Salmon, L., Schauer, J., Zeng, L., Kiang, C., Zhang, Y., Cass, G., 2005. Seasonal trends in PM2.5 source contributions in Beijing, China. Atmos. Environ. 39, 3967–3976.

Zheng, Z., Che, W., Zheng, Z., Chen, L., Zhong, L., 2013. Analysis of spatial and temporal variability of PM10 concentrations using MODIS aerosol optical thickness in the Pearl River Delta Region, China. Aerosol Air Qual. Res. 13, 862–876.